HHS Public Access

Author manuscript

*Gastroenterology*. Author manuscript; available in PMC 2021 March 01.

Published in final edited form as:

*Gastroenterology*. 2020 March ; 158(4): 985–999.e9. doi:10.1053/j.gastro.2019.11.031.

# HNF4 Regulates Fatty Acid Oxidation and is Required for Renewal of Intestinal Stem Cells in Mice

**Lei Chen**[1,2], **Roshan P. Vasoya**[1], **Natalie H. Toke**[1], **Aditya Parthasarathy**[1], **Shirley Luo**[1], **Eric Chiles**[2], **Juan Flores**[3], **Nan Gao**[3], **Edward M. Bonder**[3], **Xiaoyang Su**[2,4], **Michael P. Verzi**[1,2,5,*]

[1]Department of Genetics, Human Genetics Institute of New Jersey, Rutgers University, Piscataway, NJ 08854, USA

[2]Rutgers Cancer Institute of New Jersey, New Brunswick, NJ 08903, USA

[3]Department of Biological Sciences, Rutgers, The State University of New Jersey, Newark, NJ 07102, USA

[4]Department of Medicine, Rutgers-Robert Wood Johnson Medical School, New Brunswick, NJ 08901, USA.

[5]Rutgers Center for Lipid Research, New Brunswick, NJ 08901, USA

## Abstract

**Background & Aims:** Functions of intestinal stem cells (ISCs) are regulated by diet and metabolic pathways. Hepatocyte nuclear factor 4 (HNF4) are transcription factors that bind fatty acids. We investigated how HNF4 transcription factors regulate metabolism and their functions in ISCs in mice.

**Methods:** We performed studies with *Villin*-Cre$^{ERT2}$, *Lgr5-EGFP-IRES*-Cre$^{ERT2}$, *Hnf4a*$^{f/f}$, and *Hnf4g*$^{Crispr/Crispr}$ mice. *Villin*-Cre$^{ERT2}$; *Lgr5-EGFP-IRES*-Cre$^{ERT2}$; *Hnf4a*$^{f/f}$; *Hnf4g*$^{Crispr/Crispr}$ mice are hereafter referred to *Hnf4ag*$^{DKO}$. Mice were given tamoxifen to induce Cre recombinase. Mice transgenic with only Cre alleles (*Villin*-Cre$^{ERT2}$, *Lgr5-EGFP-IRES*-Cre$^{ERT2}$, *Hnf4a*$^{+/+}$, and *Hnf4g*$^{+/+}$) or mice given vehicle were used as controls. Crypt and villus cells were isolated, incubated with fluorescently labeled fatty acid or glucose analog, and analyzed by confocal microscopy. Fatty acid oxidation activity and tricarboxylic acid (TCA) metabolites were measured

*Correspondence: verzi@biology.rutgers.edu (M.P.V.).

Author contributions

L.C. conceived and designed the study, performed benchwork and bioinformatics, collected and analyzed the data, and wrote the manuscript; R.P.V., N.H.T., A.P., S.L., J.F., E.M.B. and N.G. contributed to benchwork. E.C. and X.Y.S. contributed to LC-MS analysis. M.P.V. conceived, designed and supervised the study, and wrote the manuscript.



Conflicts of interest

The authors declare no competing interests.

Data availability

The accession number of the Hnf4 mutants versus WT transcriptome, HNF4 ChIP-seq and H3K27ac MNase-ChIP-seq of mouse intestinal epithelial cells have been deposited in GEO (GSE112946). GSE83394 was used to analyze chromatin accessibility and RNA-seq data of Lgr5$^{+}$ intestinal stem cells.

in cells collected from the proximal half of the small intestine of *Hnf4ag*$^{DKO}$ and control mice. We performed chromatin immunoprecipitation and gene expression profiling analyses to identify genes regulated by HNF4 factors. We established organoids from duodenal crypts, incubated them with labeled palmitate or acetate, and measured production of TCA metabolites or fatty acids. Acetate, a precursor of acetyl-CoA (a product of fatty acid beta-oxidation [FAO]), or dichloroacetate, a compound that promotes pyruvate oxidation and generation of mitochondrial acetyl-CoA, were used for metabolic intervention.

**Results:** Crypt cells rapidly absorbed labeled fatty acid, and mRNA levels of Lgr5$^{+}$ stem cell markers (*Lgr5*, *Olfm4*, *Smoc2*, *Msi1*, and *Ascl2*) were downregulated in organoids incubated with etomoxir, an inhibitor of FAO, indicating that FAO was required for renewal of ISCs. HNF4A and HNF4G were expressed in ISCs and throughout the intestinal epithelium. Single knockout of either HNF4A or HNF4G did not affect maintenance of ISCs, but double-knockout of HNF4A and HNF4G resulted in ISC loss; stem cells failed to renew. FAO supports ISC renewal, and HNF4 transcription factors directly activate FAO genes, including *Acsl5* and *Acsf2* (encode regulators of acyl-CoA synthesis), *Slc27a2* (encodes a fatty acid transporter), *Fabp2* (encodes fatty acid binding protein), and *Hadh* (encodes hydroxyacyl-CoA dehydrogenase). In the intestinal epithelium of *Hnf4ag*$^{DKO}$ mice, expression levels of FAO genes, FAO activity, and metabolites of TCA were all significantly decreased, but fatty acid synthesis transcripts were increased, compared with control mice. The contribution of labeled palmitate or acetate to the TCA cycle was reduced in organoids derived from *Hnf4ag*$^{DKO}$ mice, compared with control mice. Incubation of organoids derived from double-knockout mice with acetate or dichloroacetate restored stem cells.

**Conclusions:** In mice, the transcription factors HNF4A and HNF4G regulate expression of genes required for fatty acid oxidation and are required for renewal of intestinal stem cells.

## Graphical Abstract

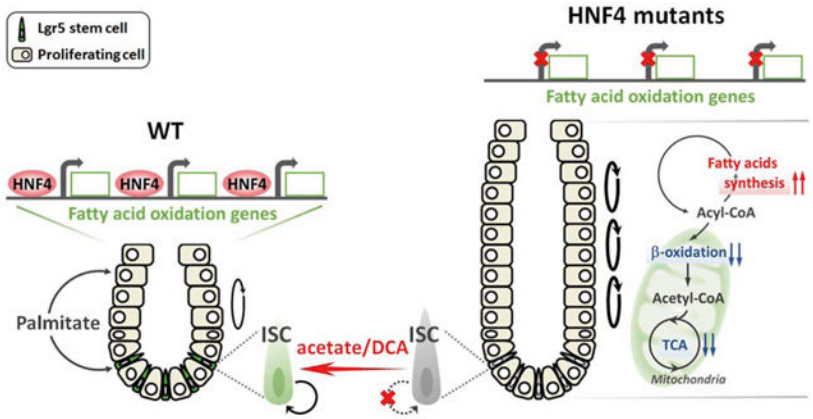


## Lay Summary:

We identified proteins that regulate metabolic processes required for intestinal stem cell renewal and replacement of the intestinal epithelium as cells die.

### Keywords

regulatory networks; stemness; mitochondria; gene expression

## Introduction

The intestinal epithelium has the capacity to self-renew and generate differentiated cells. Its turnover occurs every 3–5 days, fueled by an actively cycling stem cell population characterized by Lgr5 expression[1]. Intestinal stem cells (known as Lgr5$^+$ crypt base columnar cells or ISCs) and their proliferating progeny are nestled into cup-like structures termed crypts, while luminal projections called villi consist entirely of differentiated cells. Lgr5$^+$ ISCs function as the primary cell of origin of colon tumors[2], are essential for intestinal regeneration following injury[3], and function dynamically in response to different nutritional environments.

Nutritional regulation and metabolic control have profound roles in stem cell biology[4–8]. Studies have shown that ISCs respond to caloric restriction[9, 10] and dietary nutrients including fatty acids[11], glucose[12], N-acetyl-D-glucosamine[13] and amino acids[14, 15]. Work from our lab[16, 17] and others[18] have revealed that Lgr5$^+$ cells are particularly dependent upon mitochondrial metabolism, and others have suggested that fatty acid oxidation could fuel oxidative phosphorylation in ISCs[10]. These studies demonstrate that cellular metabolism is a fundamental regulator of intestinal stem cell homeostasis. However, it remains unclear how the unique metabolic state of intestinal stem cells is established.

Since fatty acid β-oxidation (FAO) is crucial for stem cell maintenance in multiple tissues[10, 19–22], there is a clear imperative to understand the regulatory mechanisms through which ISCs implement FAO for self-renewal. Hepatocyte nuclear factor 4 (HNF4) factors have a conserved ligand-binding domains that are constitutively bound to fatty acids[23–26]. HNF4A is an important regulator of metabolic homeostasis, and transcribes genes involved in hepatic lipid metabolism[27–29]. Genes associated with acyl-CoA metabolism were identified as putative HNF4A targets[28], and other studies have also shown that HNF4A binds acyl-CoA-binding proteins and fatty acyl-CoA thioesters[30, 31]. In *Drosophila*, dHNF4 is responsive to dietary signals, functions as a sensor for free fatty acids, and is essential for lipid catabolism and β-oxidation for energy production[32].

The intestinal stem cell has been implicated in intestinal disease and cancer. Understanding the regulatory mechanisms controlling intestinal stem cell physiology is of great importance to human health and regenerative medicine[33–37]. However, the mechanisms controlling ISC metabolism are poorly understood. Given the potential contribution of FAO in stem cell maintenance[10, 19–22] and the importance of HNF4 in regulating lipid metabolic processes[32, 38, 39], we investigated how HNF4 transcription factors impact ISC metabolism, and whether HNF4-dependent metabolic regulation is required for ISC maintenance.

## Methods

Additional experimental details on cell isolation, histology and immunostaining, western blot, RNA extraction and qRT-PCR, organoid culture, counting and immunofluorescence, FAO activity assay, fatty acid extraction and saponification, LC-MS analysis, and bioinformatics can be found in supplemental materials.

## Mice

The *Villin-Cre*$^{ERT2}$ transgene[40], *Lgr5-EGFP-IRES-Cre*$^{ERT2}$ knock-in[1], *Hnf4α*$^{f/f}$[38] and *Hnf4γ*$^{Crispr/Crispr}$[41] alleles were integrated to generate the conditional compound-mutants and controls. Experimental mice (8–12 weeks old) were treated with tamoxifen (Sigma T5648) at 50mg/kg/day or vehicle by intraperitoneal injection. To avoid the non-specific phenotype caused by tamoxifen on *Villin-Cre*$^{ERT2}$ models[42], tamoxifen-induced Cre-only controls were also tested in this study. All mouse protocols and experiments were approved by the Rutgers Institutional Animal Care and Use Committee. All samples were collected between 12:00 and 14:00 to avoid circadian variability.

## Fatty acid and glucose analog uptake

Crypt and villus cells were freshly isolated from mouse intestine as described above. Cells were incubated with different durations (0, 2, 5, 30 and 60 min, in dark, on ice) of fluorescent BODIPY™ FL C16 fatty acid (4,4-Difluoro-5,7-Dimethyl-4-Bora-3a,4a-Diaza-s-Indacene-3-Hexadecanoic Acid, also known as palmitic acid, 10 μM, Invitrogen D3821), BODIPY™ FL C12 fatty acid (4,4-Difluoro-5-(2-Thienyl)-4-Bora-3a,4a-Diaza-s-Indacene-3-Dodecanoic Acid, 10 μM, Invitrogen D3835) or 2-NBDG (2-(N-(7-Nitrobenz-2-oxa-1,3-diazol-4-yl)Amino)-2-Deoxyglucose, 10 μM, Invitrogen N13195) on a rocker. There were no obvious differences of fatty acid/glucose uptake when we compared the incubation condition on ice and at room temperature. To increase viability of isolated crypt and villus cells, cells were incubated with BODIPY™ FL C16, FL C12, or 2-NBDG on ice in this study. Trypan blue staining was used to verify cell viability throughout the experimental timecourse. After incubation, live cells were washed with PBS twice, and then stained with DraQ5 (Cell signaling 4084L) at room temperature for 5 min. Live cells were mounted and viewed on a Zeiss LSM 510 Meta confocal microscope. Only intact intestinal crypt or villus units were used to measure uptake. We noted that fixation can quench the fluorescence of fatty acid with short-term incubation (2 min and 5 min) but works fine for the long-term incubation (30 min and 60 min). When fixation was used to maintain cell morphology for next day imaging, cells were fixed with 4% paraformaldehyde at room temperature for 20 min, washed with PBS for twice, and then stained with DAPI (Biotium 40043, 1:5000) at room temperature for 5 min. After nuclear staining, cells were washed with PBS, resuspended in fluorescent mounting medium, and mounted for subsequent imaging. All images comparing tissues were acquired at the same time and using identical imaging conditions. ImageJ was used to quantify the uptake of fluorescent fatty acid/glucose analog.

## TCA metabolite extraction

Villus cells were scraped and collected from the proximal half of the small intestine of *Hnf4αγ*$^{DKO}$ mice (3 days post tamoxifen injection) and their littermate controls. Cells were resuspended in ice cold extraction buffer (40:40:20 methanol:acetonitrile:$H_2O$ with 0.5% V/V formic acid). 500 μl of extraction buffer was added per 50 mg tissue, incubated on ice for 5 min, and followed by adding 25 μl 15% (m/V) $NH_4HCO_3$. Samples were centrifuged at 15000 g for 10 min at 4°C to pellet cell debris and proteins. The supernatant was transferred into a phospholipid removal column (Phenomenex 8B-S133-TAK) for further cleanup, and

then stored at −80°C for subsequent LC-MS analysis. Tissue weight was used to normalize the corrected ion counts of TCA metabolites.

For U-$^{13}C_{16}$ palmitate organoid labeling experiments, tamoxifen (1 μM) or vehicle was added to culture medium for 12 hours on Day 3 after seeding. On Day 5, organoids were treated with 0.5 mM U-$^{13}C_{16}$ palmitate (Sigma 605573) and 1 mM carnitine (Sigma C0158) for 24 hours prior to harvesting. For U-$^{13}C_2$ acetate organoid labeling experiments, tamoxifen (1 μM) or vehicle was added to culture medium for 12 hours on Day 3 after seeding. On Day 6, organoids were treated with 2.5 mM U-$^{13}C_2$ acetate (1,2-$^{13}C_2$, Cambridge Isotope Laboratories, Inc. CLM-440–1) for 6 hours prior to harvesting. 250 μl of extraction buffer was used to extract metabolites from 10 mg of organoid pellets (10 μl pellet size ≈ 10 mg), and followed the same protocol as descried above. Protein concentration was determined by Pierce BCA Protein Assay Kit (Thermo), and was used to normalize the corrected ion counts of TCA metabolites.

### Statistical analysis

The data are presented as mean ± SEM, and statistical comparisons were performed using one-way ANOVA followed by Dunnett's post test with the GraphPad Prism version 7.02 or Student's t-test at $P < 0.001$***, $P < 0.01$** or $P < 0.05$*. Bioinformatics-related statistical analysis was done with the embedded statistics in each package, including GSEA[43], Cuffdiff[44] and HOMER[45]. $P < 0.05$ or FDR < 0.05 (95% confidence interval) was considered statistically significant.

## Results

### Disruption of FAO impairs self-renewal of ISCs

Studies have begun to delineate the impact of fatty acids on intestinal stem cell function[10, 11], yet the capacity of crypt cells to import fatty acids is unclear. Palmitic acid accounts for 20–30% of total fatty acids in humans, and can be attained from the diet or synthesized endogenously[46]. To evaluate fatty acid uptake, we isolated crypt and villus epithelial cells from mouse intestine and incubated them with fluorescent palmitic acid. Crypt cells rapidly absorbed labeled palmitic acid within 2 minutes of incubation (Figures 1A–D), and fluorescent intensity increased over time (Figure 1A and S1A). By comparison, villus cells absorbed the labeled fatty acids more slowly, lacking fluorescent signal until 30–60 minutes (Figure 1A and S1B). By contrast, a fluorescent glucose analog was absorbed by the villus compartment within 5 minutes of incubation (Figure 1E and S1C). Reports of treatment of Lgr5$^+$ stem cells with glycolysis inhibitors showed a mild effect in organoid reconstitution[18], thus leaving open a possible role for fatty acids in ISC energy metabolism. To investigate fatty acid uptake of ISCs, crypts were isolated from *Lgr5-EGFP-IRES-Cre$^{ERT2}$* knock-in[1] mice and incubated with BODIPY™ fatty acid. Red fluorescent labeled dodecanoic acid was indeed observed in Lgr5-GFP$^+$ stem cells (Figures 1D), as well as in other crypt cells. To further investigate the functional requirement of FAO in ISCs, Etomoxir, a FAO inhibitor, was applied using the well-established intestinal organoid assay[47]. Lgr5-GFP$^+$ stem cells were observed in the budding crypt domains of organoids, as expected. However, upon treatment with the FAO inhibitor, Lgr5-GFP expression

diminished in a dose-dependent manner (Figure 1F). The transcript levels of $Lgr5^+$ stem cell markers, including *Lgr5*, *Olfm4*, *Smoc2*, *Msi1* and *Ascl2*, were also dramatically downregulated with FAO inhibition by Etomoxir (Figure 1G), suggesting that FAO is required for self-renewal of ISCs[10].

## HNF4 factors directly activate FAO genes and support β-oxidation in the intestinal epithelium

HNF4A has been implicated in fatty acid metabolism, with severe lipid deposits accumulating upon conditional loss of *Hnf4a* in the liver[38]. Compared to the liver, loss of function studies of HNF4A in the intestine show relatively minor phenotypes[48–51]. We recently demonstrated that the transcription factor HNF4A acts redundantly with an intestine-restricted HNF4 paralog, HNF4G, to activate enhancer chromatin and stabilize enterocyte cell identity[41]. Expression profiling of $Hnf4a\gamma^{DKO}$ ($Hnf4a^{f/f}$; $Villin\text{-}Cre^{ERT2}$; $Hnf4\gamma^{Crispr/Crispr}$) mice indicated that the top gene ontology categories of HNF4-dependent genes are associated with lipid metabolism[41]. GSEA indicates that genes associated with lipid digestion and transport (Figure 2A), as well as fatty acid oxidation (Figure 2B and 2C), are all significantly downregulated in $Hnf4a\gamma^{DKO}$. FAO, also termed β-oxidation, refers to the sequential removal of 2-carbon units from acyl chains by oxidation at the β-carbon position. The TCA cycle utilizes acetyl-CoA derived from FAO. Together, these processes generate NADH and $FADH_2$, which fuel oxidative phosphorylation to generate ATP. In mammals, FAO occurs in both mitochondria and peroxisomes, and transcript levels of genes that function in virtually every step in the process of FAO are compromised upon loss of HNF4 factors (Figure 2D and 2E). Conversely, transcripts associated with lipogenesis are elevated in $Hnf4a\gamma^{DKO}$ epithelium (Figure 2F). Notably, genes promoting FAO are more likely to have nearby HNF4-binding sites than lipogenesis genes based upon ChIP-seq analysis (MACS $P \leq 10^{-3}$, HNF4 direct targets are indicated by asterisks in Figure 2D–F). For example, acyl-CoA synthetases catalyze the initial reaction in fatty acid metabolism by forming a thioester bond between a fatty acid and coenzyme A, and HNF4A and HNF4G directly bind to the acyl-CoA synthetase genes *Acsl5* and *Acsf2* (see HNF4 ChIP-seq tracks in Figure 2G and S2A respectively). HNF4 paralogs can also bind to other β-oxidation genes (Figure S2A), such as *Slc27a2* (fatty acid transporter), *Fabp2* (fatty acid binding) and *Hadh* (hydroxyacyl-CoA dehydrogenase). The protein encoded by *Abcd1*, a member of the superfamily of ATP-binding cassette transporters, is involved in peroxisomal import of very long chain fatty acids. In peroxisomal FAO, the first reaction is catalyzed by an acyl-CoA oxidase (ACOX), which is regarded as the main enzymatic step controlling flux through the pathway. We find HNF4A and HNF4G directly bind to *Abcd1*, *Acox1* and other important peroxisomal FAO genes including *Ehhadh* (see HNF4 ChIP-seq tracks in Figure 2H and S2A). These mitochondrial and peroxisomal β-oxidation genes are robustly expressed in WT, but are dramatically downregulated in $Hnf4a\gamma^{DKO}$ (FDR < 0.05, see RNA-seq tracks in Figure 2G, 2H, and S2). Consistent with direct activation by HNF4, accessible chromatin structure is lost at HNF4-bound regions of these β-oxidation gene loci in $Hnf4a\gamma^{DKO}$ (see MNase-H3K27ac ChIP-seq tracks in Figure 2G, 2H, and S2A).

These findings suggest that HNF4 factors directly activate genes that contribute to fatty acid catabolism (summary schematic of results in Figure S2B). We therefore measured palmitoyl-

CoA-induced enzymatic activity in cell extracts of *Hnf4α γ*$^{DKO}$ intestinal epithelium versus controls. Consistent with reduced levels of FAO gene expression, *Hnf4α γ*$^{DKO}$ epithelium exhibits impaired FAO activity compared to controls (Figure 2I). We hypothesized that compromised FAO upon HNF4 loss therefore leads to a subsequent reduction in TCA metabolites. Indeed, TCA metabolites of villus cells were reduced in *Hnf4α γ*$^{DKO}$, indicated by LC-MS measurements of α-ketoglutarate, succinate, fumarate and malate (Figure 2J). In addition to fatty acid oxidation, acetyl-CoA can be generated by glycolysis, followed by pyruvate oxidation in the mitochondria. However, neither glycolysis pathway transcripts nor genes contributing to pyruvate oxidation are compromised upon HNF4 loss (Figure S3). Taken together, HNF4 paralogs bind to and activate FAO genes, and loss of HNF4 leads to compromised transcript levels of FAO genes, impaired palmitoyl-CoA dependent enzymatic activity, and reduced levels of TCA metabolites.

## Loss of HNF4 paralogs in the intestinal epithelium triggers Lgr5$^{+}$ stem cell loss

Since HNF4 factors appear to contribute strongly to β-oxidation, a process important for intestinal stem cell renewal[10], we next explored whether HNF4 factors could be contributing to ISC function. We applied DNA-binding motif analysis to ATAC-seq data of isolated ISCs[52] and found that the HNF4A/G motif is the top-scoring factor (Figure 3A), suggesting that HNF4 factors could function as broad regulators of gene expression in ISCs. RNA-seq data of ISCs[52] demonstrate high *Hnf4α* and *Hnf4γ* expression in the Lgr5$^{+}$ intestinal stem cells (Figure 3B). Immunoreactivity of HNF4A and HNF4G was observed throughout the intestinal epithelium, including in crypt base columnar stem cells (Figure 3C). On the *Hnf4γ* mutant background, induced deletion of *Hnf4α* throughout the intestinal epithelium using the *Villin-Cre*$^{ERT2}$ driver (Figure S4A) triggers loss of stem cells within 4 days of tamoxifen treatment, as indicated by the absence of OLFM4-expressing cells at the base of crypts throughout the intestine (Figure 3D and S4B). However, single knockout of either HNF4A or HNF4G does not affect the maintenance of intestinal stem cells (Figure 3D), suggesting redundant functions of HNF4 paralogs in stem cell renewal. Reduced Lgr5$^{+}$ stem cell transcripts, *Lgr5*, *Olmf4*, *Smoc2*, *Msi1* and *Ascl2*, are observed in the crypts of *Hnf4α γ*$^{DKO}$ at day 2 post tamoxifen induced knockout (Figure 3E), and *Hnf4α γ*$^{DKO}$ mice had to be euthanized within 5 days due to compromised epithelial functions. To further monitor the Lgr5-expressing cell population, we generated mice in which we could both inactivate HNF4 throughout the epithelium and visualize the Lgr5-expressing stem cells with an Lgr5-GFP knock-in allele[1]: *Lgr5-EGFP-IRES-Cre*$^{ERT2}$*; Villin-Cre*$^{ERT2}$; *Hnf4α*$^{f/f}$; *Hnf4γ*$^{Crispr/Crispr}$. Consistent with OLFM4 staining, there are no detectible Lgr5-GFP$^{+}$ stem cells remaining in the *Hnf4α γ*$^{DKO}$ mice at day 4 after tamoxifen treatment (Figure 3F and S4C).

To test for a cell-autonomous role for HNF4 in stem cells, we inactivated HNF4 using the *Lgr5-EGFP-Cre*$^{ERT2}$, a stem cell-specific Cre driver that is mosaically expressed in a subset of crypts[1]. HNF4A-negative cells are observed in the crypts and villi of *Lgr5-EGFP-Cre*$^{ERT2}$; *Hnf4α*$^{f/f}$; *Hnf4γ*$^{+/-}$ mice after 5 days and 10 days post tamoxifen treatment, indicating efficient knockout of HNF4A in the stem cells and their progeny. However, most HNF4 recombination is not preserved in *Lgr5-EGFP-Cre*$^{ERT2}$; *Hnf4α γ*$^{DKO}$ mice, implying that the mutant stem cells are replaced by neighboring non-recombined healthy cells. These

findings suggest that HNF4 factors are required in the ISCs in a cell-autonomous fashion (Figure 3G and S4D). We also find increased apoptosis in *Hnf4aγ*$^{DKO}$ (Figure 3H), particularly in the crypt base (Figure 3I), corresponding to loss of stem cell survival without HNF4.

We utilized the organoid model to investigate the role of HNF4 in Lgr5$^{+}$ stem cells. Organoids derived from *Hnf4aγ*$^{DKO}$ crypts after 2 days of tamoxifen injection do not establish viable cultures (Figure S4E), so we derived organoids from uninjected *Lgr5-EGFP-Cre*$^{ERT2}$*; Villin-Cre*$^{ERT2}$; *Hnf4a*$^{f/f}$; *Hnf4γ*$^{Crispr/Crispr}$ crypts and treated with tamoxifen *in vitro*. Unlike wild type organoids, which grow indefinitely with branched crypt domains containing Lgr5$^{+}$ stem cells, *Hnf4aγ*$^{DKO}$ organoids initially form spherical organoids, but die out after passaging (Figure 4A and 4B). Live imaging of Lgr5-GFP in *Hnf4aγ*$^{DKO}$ organoids reveals diminished Lgr5-GFP$^{+}$ cells compared to controls (Figure 4A and S4F), suggesting HNF4 factors are also required to maintain Lgr5 stem cells in organoid cultures. We hypothesized that the absence of HNF4 could skew the balance of a stem cell's decision to renew versus enter the proliferating cell population towards lineage commitment. Knockout of HNF4 resulted in spherical organoids homogeneously composed of proliferative cells, as revealed by EdU and Ki67 staining (Figure 4C). Consistent with this phenotype, expression of Lgr5 stem cell markers is downregulated (Figure 4D), whereas the expression of proliferative cell markers is upregulated (Figure 4E). As with the *in vitro* data, *in vivo* data suggest that loss of HNF4 factors triggers a burst in cell proliferation, crypt expansion, and an increased population of Ki67$^{+}$ cells by day 4 after tamoxifen treatment (Figure 4F), coincident with the timing of stem cell loss. This finding is corroborated by elevated transcript levels of proliferative cell markers observed in *Hnf4aγ*$^{DKO}$ mice (Figure 4G). Taken together, both *in vitro* (Figure 4A–E) and *in vivo* (Figure 4F and 4G) data suggest that in the absence of HNF4 paralogs, stem cells fail to renew and instead contribute to a population of proliferating cells, presumably representing the transit-amplifying population.

## ISCs lacking HNF4 paralogs are rescued by metabolic intervention

The importance of FAO in stem cell maintenance has been reported in several tissues[10, 19–22], and corroborated in this study (Figure 1). Since we found that HNF4 factors bind to and activate FAO genes (Figure 2 and Figure S2), we examined whether the contribution of U-$^{13}C_{16}$ palmitate to TCA cycle metabolites was altered in *Hnf4aγ*$^{DKO}$ organoids (schematic see Figure 5A and 5B). Indeed, contribution of labeled palmitate to the TCA cycle was substantially reduced in *Hnf4aγ*$^{DKO}$ organoids (Figure 5C and Figure S5A), consistent with diminished FAO activity in HNF4 mutants. To determine the fate of acetate (a precursor of acetyl-CoA, a major product pf FAO) in *Hnf4aγ*$^{DKO}$ mutants, we cultured primary organoids with U-$^{13}C_2$ acetate for 6 hours, and measured the incorporation of $^{13}$C in TCA metabolites as well as in saponified lipid (schematic see Figure 5A and 5B). $^{13}$C-labeled TCA metabolites were indeed reduced in *Hnf4aγ*$^{DKO}$ mutants compared to the WT organoids (Figure 5Dand Figure S5B). In contrast, there was a stark increase in the $^{13}$C incorporation in fatty acid synthesis in *Hnf4aγ*$^{DKO}$ mutants (Figure 5E). These data suggest that HNF4 loss redirects acetyl-CoA away from the TCA cycle and towards fatty acid synthesis.

To test whether impaired FAO in the *Hnf4α γ*$^{DKO}$ was contributing to stem cell loss, we tested whether mutant organoids were sensitized to FAO inhibition by Etomoxir (schematic see Figure 6A). *Hnf4α γ*$^{DKO}$ organoids take on a spherical morphology consisting of proliferative cells and a lack of Lgr5$^{+}$-cells (Figure 4A and Figure 4C). FAO inhibition accelerates the formation of spherical organoids in *Hnf4α γ*$^{DKO}$ within 24 hours in the presence of Etomoxir (Figure S5C and S5D). If a FAO defect was responsible for stem cell loss in *Hnf4α γ*$^{DKO}$ organoids, we wondered whether supplement of acetate could rescue the phenotype (schematic see Figure 6A and 6B). Lower doses of acetate treatment (2.5 mM) could not rescue the spherical organoid structure but did induce visible Lgr5-GFP fluorescence compared to the untreated group. Higher doses of acetate, approaching levels observed in the colonic lumen[53], rescued both the spherical morphology and expression of the Lgr5-GFP reporter in *Hnf4α γ*$^{DKO}$ organoids (Figure 6C, top panel). More than 80% of *Hnf4α γ*$^{DKO}$ organoids exhibited stem cell-deficient, spherical structures upon Hnf4 loss, but acetate rescued the organoid morphology, with only 10% of *Hnf4α γ*$^{DKO}$ organoids showing spherical structures after 25 mM acetate treatment (Figure 6D), forestalling the collapse of the *Hnf4α γ*$^{DKO}$ organoids for several days. Corroborating these findings, the transcript levels of Lgr5 stem cell markers are also rescued upon acetate treatment in *Hnf4α γ*$^{DKO}$ (Figure 6E).

Disruption of FAO in HNF4 mutants, and subsequent rescue of stem cell renewal by acetate suggested that a deficiency in acetyl-CoA could be limiting stem cell renewal. Pyruvate oxidation is an alternative source of acetyl-CoA for the TCA cycle. As pyruvate oxidation genes were not compromised in *Hnf4α γ*$^{DKO}$ (Figure S3), we tested whether dichloroacetate (DCA), a compound promoting pyruvate oxidation and generation of mitochondrial acetyl-CoA (schematic see Figure 6A and 6B) could also rescue the *Hnf4α γ*$^{DKO}$ mutant phenotype. Indeed, treatment with DCA also rescued stem cell loss in *Hnf4α γ*$^{DKO}$ (Figure 6C, bottom panel, 6D and 6F). Interestingly, the rescue dose of acetate (25 mM) or DCA (10 mM) that prolongs stem cell maintenance in *Hnf4α γ*$^{DKO}$ mutant organoids impairs the growth of WT organoids (Figure S5E–G).

Exogenous acetate supplementation has been shown to rescue cellular functions dependent upon FAO by substituting for acetyl-CoA[54–56]. Given that FAO and TCA metabolites are reduced in *Hnf4α γ*$^{DKO}$ mutants (Figure 2, 5C, 5D and Figure S2, S5A, S5B), we wondered whether elevated levels of acetate could rescue stem cell function in *Hnf4α γ*$^{DKO}$ organoids by supporting the TCA cycle. Indeed, acetate supplementation restored TCA metabolite levels in *Hnf4α γ*$^{DKO}$ (Figure 6G). In summary, we demonstrate that FAO promotes stem cell renewal. HNF4 factors bind to and activate FAO genes, and upon loss of HNF4 factors, fatty acid synthesis is elevated at the expense of β-oxidation. Acetate supplementation suppresses stem cell loss in the *Hnf4α γ*$^{DKO}$, suggesting that HNF4 factors may be required for stem cell renewal via their role in promoting β-oxidation.

## Discussion

Disruption of FAO results in hematopoietic stem cell (HSC) exhaustion and lineage commitment of HSC daughter cells[22]. Quiescent neural stem and progenitor cells (NSPCs) require high levels of FAO, and FAO inhibition induces NSPCs exit from quiescence to

proliferation[57]. Together with our work and recent findings, there is an emerging theme that links FAO to stem cell maintenance. Conditions leading to elevated fatty acid levels and mitochondrial metabolism correspond to enhanced ISC renewal: Fasting augments ISC numbers by shifting metabolism toward more FAO, whereas chronic disruption of *Cpt1a*, the rate-limiting enzyme in FAO, decreases ISC numbers and function[10]. Meanwhile, a high-fat diet elevates $Lgr5^+$ cell numbers, and culturing with fatty acids bolsters self-renewal of intestinal organoids[11]. $Lgr5^+$ ISCs exhibit high mitochondrial activity, and inhibition of mitochondrial activity in $Lgr5^+$ ISCs leads to compromised stem cell function[16–18]. Collectively, these studies imply that the high mitochondrial content of ISCs[12, 18] is likely coordinated with a requirement for fatty acid oxidation. Our studies now provide a regulatory link through which intestinal transcription factors promote expression of genes that provide the metabolic infrastructure to carry out FAO.

Glucose and fatty acids are two major fuels that drive ATP production for energy requirement. Fatty acid oxidation and pyruvate oxidation may have opposing effects on renewal of intestinal $Lgr5^+$ stem cells; inhibition of pyruvate oxidation enhances stem cell maintenance[12], whereas activation of fatty acid oxidation promotes stem cell renewal[10, 11]. Our findings suggest FAO is required for ISC renewal under normal conditions (Figure 1). Limiting mitochondrial pyruvate metabolism via genetic ablation of the mitochondrial pyruvate carrier has been shown to enhance ISC proliferation[12]. However, DCA treatment, which promotes pyruvate oxidation, restores stem cell renewal in the $Hnf4a\gamma^{DKO}$. We suspect that DCA treatment has this effect under conditions of dramatic FAO deficiency, as we observe in $Hnf4a\gamma^{DKO}$ cells (Figure 2 and Figure S2). The $Hnf4a\gamma^{DKO}$ stem cell can partially restore acetyl-CoA that is limited by loss of FAO via elevated pyruvate oxidation upon DCA treatment, which could thus help restore ISC renewal.

In our previous study[41], we observed an expansion of the crypt domain in $Hnf4a\gamma^{DKO}$ mice, which may be attributed to both an increased contribution of ISCs to the progenitor domain (this study) and a failure of crypt cells to differentiate into enterocytes[41]. Our current study finds that HNF4 transcription factors are essential for intestinal stem cell renewal, and thus provides a link between the fundamental transcriptional regulatory networks governing intestinal identity[41, 58, 59], with a metabolic program essential for intestinal stem cell function. The critical role for HNF4 factors in intestinal stem cell renewal was not previously appreciated in single HNF4 mutants due to redundancy between *Hnf4α* and *Hnf4γ* paralogs. These unappreciated HNF4 functions broaden our understanding of metabolic regulation in intestinal stem cell homeostasis, and may provide a regulatory conduit for ISCs during conditions in which elevated free fatty acids are present (such as during fasting or in the presence of high fat diet).

## Supplementary Material

Refer to Web version on PubMed Central for supplementary material.

## Acknowledgments

We thank Noriko Goldsmith and Josh Thackray for helpful imaging support.

Funding

This research was funded by a grant from the NIH (R01CA190558, M.P.V.). M.P.V is also supported by the Intestinal Stem Cell Consortium from the National Institute of Diabetes and Digestive and Kidney Diseases (NIDDK) and National Institute of Allergy and Infectious Diseases (NIAID) of the National Institutes of Health under grant number U01 DK103141. The content is solely the responsibility of the authors and does not necessarily represent the official views of the National Institutes of Health. E.M.B. was kindly supported by a Rutgers Newark Chancellor's SEED grant. Support was also received from the Sequencing Facility and Metabolomics Shared Resource of the Rutgers Cancer Institute of New Jersey (P30CA072720) and imaging core facility of Human Genetics Institute of New Jersey. L.C. was supported by New Jersey Commission on Cancer Research grant (DFHS18PPC051). R.P.V., N.H.T., A.P. and S.L. were supported by MacMillan Summer Undergraduate Research Fellowships.

## Abbreviations used in this paper:

| | |
|---|---|
| **ACOX** | acyl-CoA oxidase |
| **ATAC-seq** | assay for transposase accessible chromatin sequencing |
| **ChIP** | chromatin immunoprecipitation |
| **CPT1** | carnitine palmitoyltransferase I |
| **DAB** | 3,3'-diaminobenzidine |
| **DCA** | dichloroacetate |
| **FAO** | fatty acid β-oxidation |
| **FDR** | false discovery rate |
| **FPKM** | fragments per kilobase of transcript per million mapped reads |
| **GSEA** | gene set enrichment analysis |
| **Hadh** | hydroxyacyl-CoA dehydrogenase |
| **HNF4A** | hepatocyte nuclear factor 4 alpha |
| **HNF4G** | hepatocyte nuclear factor 4 gamma |
| **HSC** | hematopoietic stem cell |
| **IGV** | integrative genomics viewer |
| **IHC** | immunohistochemistry |
| **ISC** | intestinal stem cell |
| **LC-MS** | liquid chromatography-mass spectrometry |
| **Lgr5** | leucine rich repeat containing G protein-coupled receptor 5 |
| **MACS** | model-based analysis of ChIP-Seq |
| **MNase** | micrococcal nuclease |
| **NSPCs** | neural stem and progenitor cells |

| | |
|---|---|
| **PDH** | pyruvate dehydrogenase |
| **PDK** | pyruvate dehydrogenase kinase |
| **qRT-PCR** | quantitative reverse transcription polymerase chain reaction |
| **TCA** | tricarboxylic acid |
| **TSSs** | transcription start sites |
| **UHPLC** | ultra-high-performance liquid chromatography |

## References


1. Barker N, van Es JH, Kuipers J, et al. Identification of stem cells in small intestine and colon by marker gene Lgr5. Nature 2007;449:1003–7. [PubMed: 17934449]
2. Barker N, Ridgway RA, van Es JH, et al. Crypt stem cells as the cells-of-origin of intestinal cancer. Nature 2009;457:608–11. [PubMed: 19092804]
3. Metcalfe C, Kljavin NM, Ybarra R, et al. Lgr5+ stem cells are indispensable for radiation-induced intestinal regeneration. Cell Stem Cell 2014;14:149–59. [PubMed: 24332836]
4. Mihaylova MM, Sabatini DM, Yilmaz OH. Dietary and metabolic control of stem cell function in physiology and cancer. Cell Stem Cell 2014;14:292–305. [PubMed: 24607404]
5. Wei P, Dove KK, Bensard C, et al. The Force Is Strong with This One: Metabolism (Over)powers Stem Cell Fate. Trends Cell Biol 2018;28:551–559. [PubMed: 29555207]
6. Shyh-Chang N, Ng HH. The metabolic programming of stem cells. Genes Dev 2017;31:336–346. [PubMed: 28314766]
7. Shim J, Gururaja-Rao S, Banerjee U. Nutritional regulation of stem and progenitor cells in Drosophila. Development 2013;140:4647–56. [PubMed: 24255094]
8. Alonso S, Yilmaz OH. Nutritional Regulation of Intestinal Stem Cells. Annu Rev Nutr 2018;38:273–301. [PubMed: 29799767]
9. Yilmaz OH, Katajisto P, Lamming DW, et al. mTORC1 in the Paneth cell niche couples intestinal stem-cell function to calorie intake. Nature 2012;486:490–5. [PubMed: 22722868]
10. Mihaylova MM, Cheng CW, Cao AQ, et al. Fasting Activates Fatty Acid Oxidation to Enhance Intestinal Stem Cell Function during Homeostasis and Aging. Cell Stem Cell 2018;22:769–778 e4. [PubMed: 29727683]
11. Beyaz S, Mana MD, Roper J, et al. High-fat diet enhances stemness and tumorigenicity of intestinal progenitors. Nature 2016;531:53–8. [PubMed: 26935695]
12. Schell JC, Wisidagama DR, Bensard C, et al. Control of intestinal stem cell function and proliferation by mitochondrial pyruvate metabolism. Nat Cell Biol 2017;19:1027–1036. [PubMed: 28812582]
13. Mattila J, Kokki K, Hietakangas V, et al. Stem Cell Intrinsic Hexosamine Metabolism Regulates Intestinal Adaptation to Nutrient Content. Dev Cell 2018;47:112–121 e3. [PubMed: 30220570]
14. Deng H, Gerencser AA, Jasper H. Signal integration by Ca(2+) regulates intestinal stem-cell activity. Nature 2015;528:212–7. [PubMed: 26633624]
15. Obata F, Tsuda-Sakurai K, Yamazaki T, et al. Nutritional Control of Stem Cell Division through S-Adenosylmethionine in Drosophila Intestine. Dev Cell 2018;44:741–751 e3. [PubMed: 29587144]
16. Perekatt AO, Valdez MJ, Davila M, et al. YY1 is indispensable for Lgr5+ intestinal stem cell renewal. Proc Natl Acad Sci U S A 2014;111:7695–700. [PubMed: 24821761]
17. Srivillibhuthur M, Warder BN, Toke NH, et al. TFAM is required for maturation of the fetal and adult intestinal epithelium. Dev Biol 2018;439:92–101. [PubMed: 29684311]
18. Rodriguez-Colman MJ, Schewe M, Meerlo M, et al. Interplay between metabolic identities in the intestinal crypt supports stem cell function. Nature 2017;543:424–427. [PubMed: 28273069]

19. Xie Z, Jones A, Deeney JT, et al. Inborn Errors of Long-Chain Fatty Acid beta-Oxidation Link Neural Stem Cell Self-Renewal to Autism. Cell Rep 2016;14:991–999. [PubMed: 26832401]
20. Ryall JG, Dell'Orso S, Derfoul A, et al. The NAD(+)-dependent SIRT1 deacetylase translates a metabolic switch into regulatory epigenetics in skeletal muscle stem cells. Cell Stem Cell 2015;16:171–83. [PubMed: 25600643]
21. Stoll EA, Makin R, Sweet IR, et al. Neural Stem Cells in the Adult Subventricular Zone Oxidize Fatty Acids to Produce Energy and Support Neurogenic Activity. Stem Cells 2015;33:2306–19. [PubMed: 25919237]
22. Ito K, Carracedo A, Weiss D, et al. A PML-PPAR-delta pathway for fatty acid oxidation regulates hematopoietic stem cell maintenance. Nat Med 2012;18:1350–8. [PubMed: 22902876]
23. Chandra V, Huang P, Potluri N, et al. Multidomain integration in the structure of the HNF-4alpha nuclear receptor complex. Nature 2013;495:394–8. [PubMed: 23485969]
24. Dhe-Paganon S, Duda K, Iwamoto M, et al. Crystal structure of the HNF4 alpha ligand binding domain in complex with endogenous fatty acid ligand. J Biol Chem 2002;277:37973–6. [PubMed: 12193589]
25. Duda K, Chi YI, Shoelson SE. Structural basis for HNF-4alpha activation by ligand and coactivator binding. J Biol Chem 2004;279:23311–6. [PubMed: 14982928]
26. Wisely GB, Miller AB, Davis RG, et al. Hepatocyte nuclear factor 4 is a transcription factor that constitutively binds fatty acids. Structure 2002;10:1225–34. [PubMed: 12220494]
27. Bolotin E, Liao H, Ta TC, et al. Integrated approach for the identification of human hepatocyte nuclear factor 4alpha target genes using protein binding microarrays. Hepatology 2010;51:642–53. [PubMed: 20054869]
28. Fang B, Mane-Padros D, Bolotin E, et al. Identification of a binding motif specific to HNF4 by comparative analysis of multiple nuclear receptors. Nucleic Acids Res 2012;40:5343–56. [PubMed: 22383578]
29. Watt AJ, Garrison WD, Duncan SA. HNF4: a central regulator of hepatocyte differentiation and function. Hepatology 2003;37:1249–53. [PubMed: 12774000]
30. Hertz R, Magenheim J, Berman I, et al. Fatty acyl-CoA thioesters are ligands of hepatic nuclear factor-4alpha. Nature 1998;392:512–6. [PubMed: 9548258]
31. Petrescu AD, Payne HR, Boedecker A, et al. Physical and functional interaction of Acyl-CoA-binding protein with hepatocyte nuclear factor-4 alpha. J Biol Chem 2003;278:51813–24. [PubMed: 14530276]
32. Palanker L, Tennessen JM, Lam G, et al. Drosophila HNF4 regulates lipid mobilization and beta-oxidation. Cell Metab 2009;9:228–39. [PubMed: 19254568]
33. Barker N Adult intestinal stem cells: critical drivers of epithelial homeostasis and regeneration. Nat Rev Mol Cell Biol 2014;15:19–33. [PubMed: 24326621]
34. Bitar KN, Zakhem E. Bioengineering the gut: future prospects of regenerative medicine. Nat Rev Gastroenterol Hepatol 2016;13:543–56. [PubMed: 27507104]
35. Nakamura T, Sato T. Advancing Intestinal Organoid Technology Toward Regenerative Medicine. Cell Mol Gastroenterol Hepatol 2018;5:51–60. [PubMed: 29204508]
36. Vermeulen L, Snippert HJ. Stem cell dynamics in homeostasis and cancer of the intestine. Nat Rev Cancer 2014;14:468–80. [PubMed: 24920463]
37. Yousefi M, Li L, Lengner CJ. Hierarchy and Plasticity in the Intestinal Stem Cell Compartment. Trends Cell Biol 2017;27:753–764. [PubMed: 28732600]
38. Hayhurst GP, Lee YH, Lambert G, et al. Hepatocyte nuclear factor 4alpha (nuclear receptor 2A1) is essential for maintenance of hepatic gene expression and lipid homeostasis. Mol Cell Biol 2001;21:1393–403. [PubMed: 11158324]
39. Odom DT, Zizlsperger N, Gordon DB, et al. Control of pancreas and liver gene expression by HNF transcription factors. Science 2004;303:1378–81. [PubMed: 14988562]
40. el Marjou F, Janssen KP, Chang BH, et al. Tissue-specific and inducible Cre-mediated recombination in the gut epithelium. Genesis 2004;39:186–93. [PubMed: 15282745]
41. Chen L, Toke NH, Luo S, et al. A reinforcing HNF4-SMAD4 feed-forward module stabilizes enterocyte identity. Nat Genet 2019;51:777–785. [PubMed: 30988513]

42. Bohin N, Carlson EA, Samuelson LC. Genome Toxicity and Impaired Stem Cell Function after Conditional Activation of CreER(T2) in the Intestine. Stem Cell Reports 2018;11:1337–1346. [PubMed: 30449703]
43. Subramanian A, Tamayo P, Mootha VK, et al. Gene set enrichment analysis: a knowledge-based approach for interpreting genome-wide expression profiles. Proc Natl Acad Sci U S A 2005;102:15545–50. [PubMed: 16199517]
44. Trapnell C, Roberts A, Goff L, et al. Differential gene and transcript expression analysis of RNA-seq experiments with TopHat and Cufflinks. Nat Protoc 2012;7:562–78. [PubMed: 22383036]
45. Heinz S, Benner C, Spann N, et al. Simple combinations of lineage-determining transcription factors prime cis-regulatory elements required for macrophage and B cell identities. Mol Cell 2010;38:576–89. [PubMed: 20513432]
46. Carta G, Murru E, Banni S, et al. Palmitic Acid: Physiological Role, Metabolism and Nutritional Implications. Front Physiol 2017;8:902. [PubMed: 29167646]
47. Sato T, Vries RG, Snippert HJ, et al. Single Lgr5 stem cells build crypt-villus structures in vitro without a mesenchymal niche. Nature 2009;459:262–5. [PubMed: 19329995]
48. Babeu JP, Darsigny M, Lussier CR, et al. Hepatocyte nuclear factor 4alpha contributes to an intestinal epithelial phenotype in vitro and plays a partial role in mouse intestinal epithelium differentiation. Am J Physiol Gastrointest Liver Physiol 2009;297:G124–134. [PubMed: 19389805]
49. Cattin AL, Le Beyec J, Barreau F, et al. Hepatocyte nuclear factor 4alpha, a key factor for homeostasis, cell architecture, and barrier function of the adult intestinal epithelium. Mol Cell Biol 2009;29:6294–308. [PubMed: 19805521]
50. San Roman AK, Aronson BE, Krasinski SD, et al. Transcription factors GATA4 and HNF4A control distinct aspects of intestinal homeostasis in conjunction with transcription factor CDX2. J Biol Chem 2015;290:1850–60. [PubMed: 25488664]
51. Verzi MP, Shin H, San Roman AK, et al. Intestinal master transcription factor CDX2 controls chromatin access for partner transcription factor binding. Mol Cell Biol 2013;33:281–92. [PubMed: 23129810]
52. Jadhav U, Saxena M, O'Neill NK, et al. Dynamic Reorganization of Chromatin Accessibility Signatures during Dedifferentiation of Secretory Precursors into Lgr5+ Intestinal Stem Cells. Cell Stem Cell 2017;21:65–77 e5. [PubMed: 28648363]
53. den Besten G, van Eunen K, Groen AK, et al. The role of short-chain fatty acids in the interplay between diet, gut microbiota, and host energy metabolism. J Lipid Res 2013;54:2325–40. [PubMed: 23821742]
54. Schoors S, Bruning U, Missiaen R, et al. Fatty acid carbon is essential for dNTP synthesis in endothelial cells. Nature 2015;520:192–U113. [PubMed: 25830893]
55. Wong BW, Wang X, Zecchin A, et al. The role of fatty acid beta-oxidation in lymphangiogenesis. Nature 2017;542:49–54. [PubMed: 28024299]
56. Xiong J, Kawagishi H, Yan Y, et al. A Metabolic Basis for Endothelial-to-Mesenchymal Transition. Mol Cell 2018;69:689–698 e7. [PubMed: 29429925]
57. Knobloch M, Pilz GA, Ghesquiere B, et al. A Fatty Acid Oxidation-Dependent Metabolic Shift Regulates Adult Neural Stem Cell Activity. Cell Rep 2017;20:2144–2155. [PubMed: 28854364]
58. Lindeboom RG, van Voorthuijsen L, Oost KC, et al. Integrative multi-omics analysis of intestinal organoid differentiation. Mol Syst Biol 2018;14:e8227. [PubMed: 29945941]
59. Davison JM, Lickwar CR, Song L, et al. Microbiota regulate intestinal epithelial gene expression by suppressing the transcription factor Hepatocyte nuclear factor 4 alpha. Genome Res 2017;27:1195–1206. [PubMed: 28385711]

**What you need to know:**

**BACKGROUND AND CONTEXT:**

Nutritional and metabolic changes can alter intestinal stem cell numbers and their ability to renew. Hepatocyte nuclear factor 4 (HNF4) proteins are transcription factors that regulate hundreds of genes in the intestinal epithelium. HNF4 factors are expressed in intestinal stem cells, but their function in intestinal stem cells is unclear.

**NEW FINDINGS:**

In mice, the transcription factors HNF4A and HNF4G directly activated genes that regulate fatty acid oxidation and are required for renewal of intestinal stem cells.

**LIMITATIONS:**

The inability of intestinal stem cells in mice with double knockout of HNF4A and HNF4G to survive long term made it difficult to collect and study these cells.

**IMPACT:**

We identified HNF4 transcription factors regulate intestinal stem cell renewal and metabolic pathways required for intestinal stem cell functions.

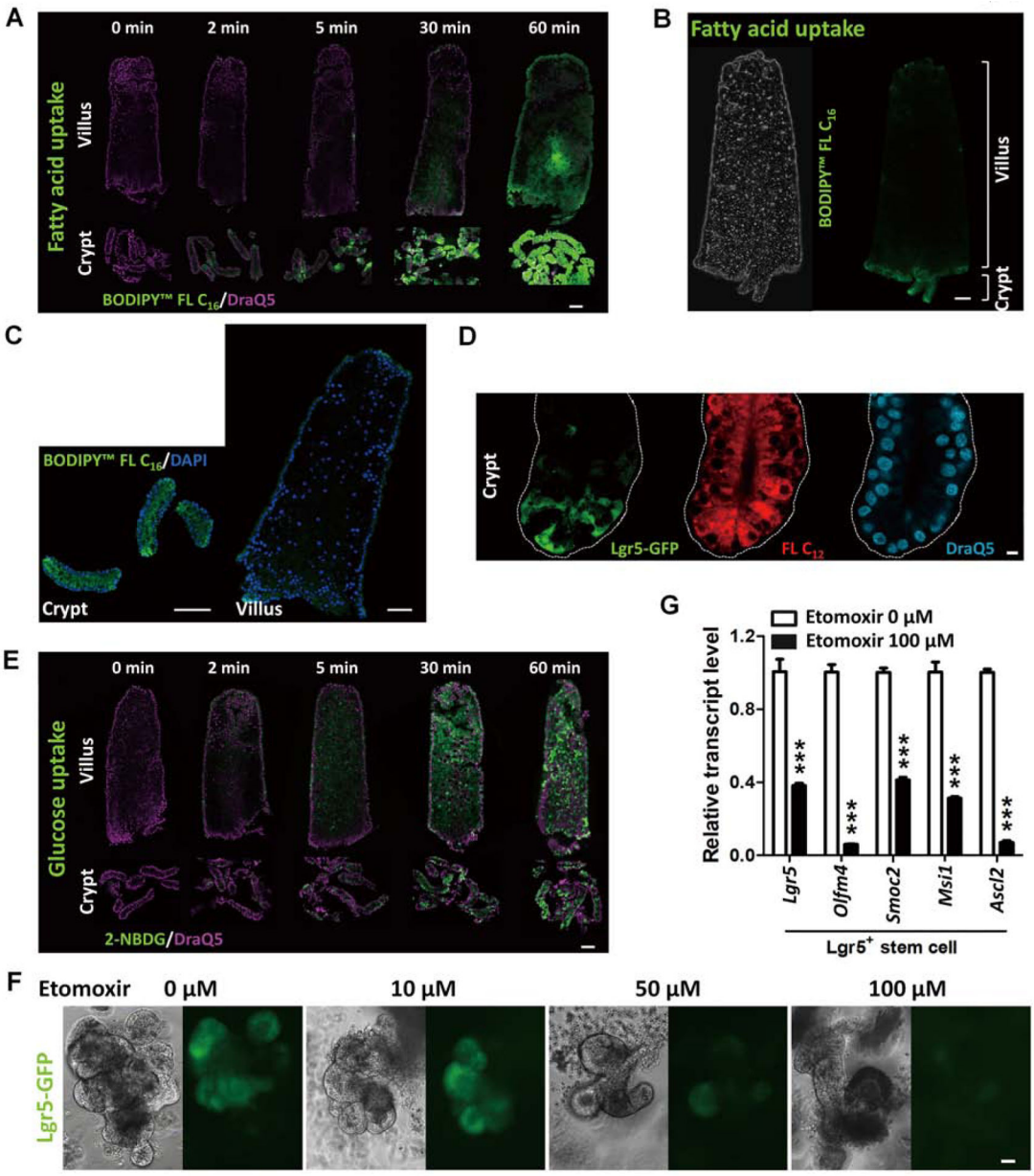


**Figure 1. FAO is required for intestinal stem cell renewal.**

(A-E) Intestinal crypts uptake fatty acid more readily than villi (n=3 independent experiments). Crypt and villus epithelial cells were isolated from the proximal half of the small intestine (from the midpoint between gastroduodenal junction to ileal-cecal junction) and incubated with 10 μM BODIPY™ FL C16 (fluorescent palmitic acid), FL C12 (fluorescent dodecanoic acid), or 10 μM 2-NBDG (fluorescent glucose analog), respectively. Similar results are seen in duodenum, jejunum and ileum (Fig. S1B). (A) Time-course study of fluorescent fatty acid (BODIPY™ FL C16) uptake shows that intestinal crypt cells uptake more fatty acid than villus cells (scale bar, 50 μm). (B-C) Fatty acid (green fluorescence) accumulates more in the crypt cells than in villus cells (scale bars, 50 μm). (D) Red fluorescent fatty acids (10 μM BODIPY™ FL C12, 5 min) are observed in Lgr5-GFP stem

cells in the crypts (scale bar, 5 μm). (E) Glucose uptake in crypt and villus cells (scale bar, 50 μm). (F) Fewer Lgr5-GFP cells are observed in organoids treated with Etomoxir (fatty acid oxidation inhibitor) for 72 hours (n=3 independent experiments). (G) qRT-PCR shows a significant decrease in the transcript levels of intestinal $Lgr5^+$ stem cell markers in the organoids treated with 100 μM Etomoxir for 72 hours. Data are presented as mean ± SEM (n=3–4 independent organoid cultures per treatment, Student's t-test, two-sided at $P < 0.001$***).

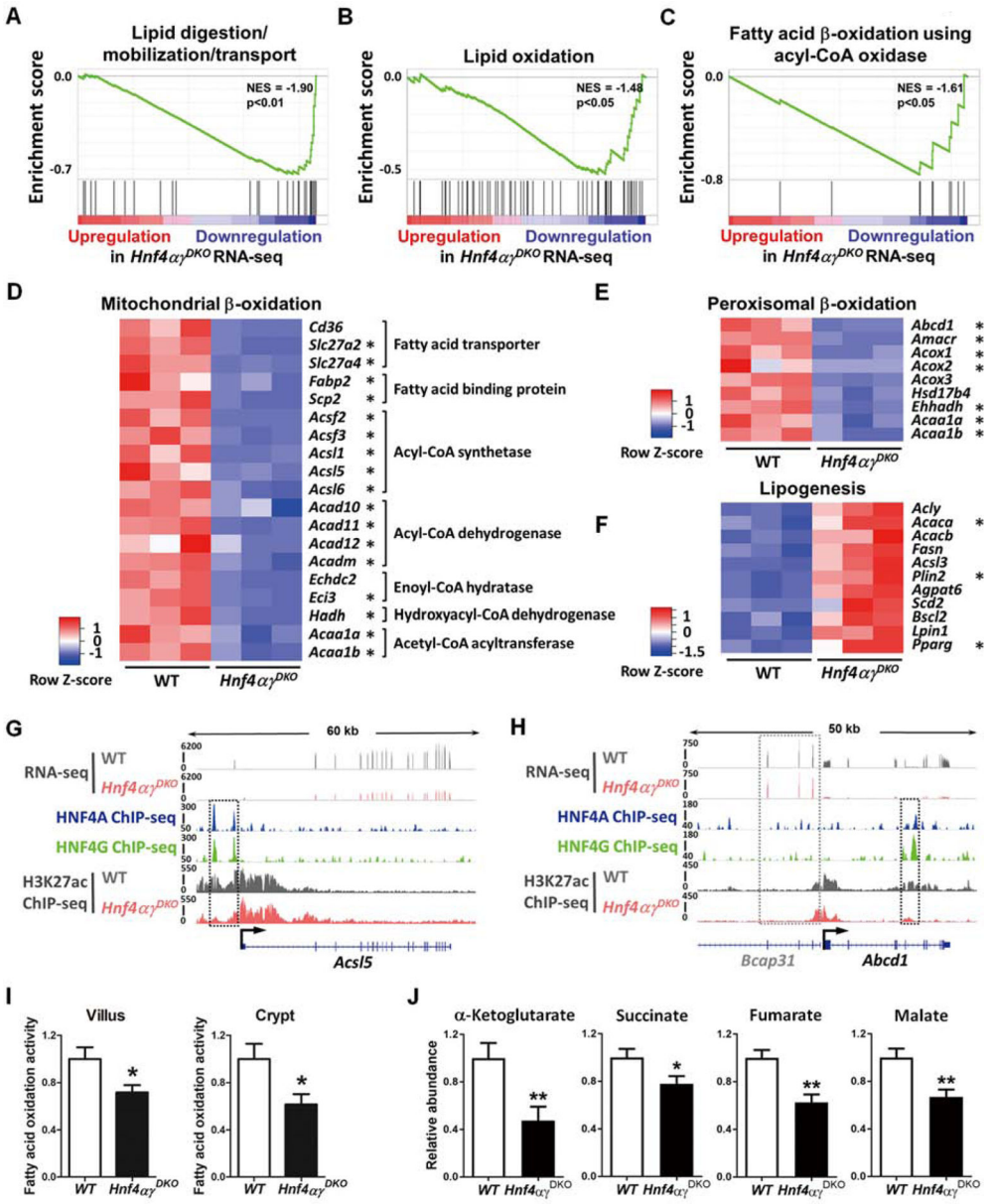


**Figure 2. HNF4 paralogs bind to and activate FAO genes, and FAO is compromised upon HNF4 loss.**

(A-C) GSEA of RNA-seq (duodenal epithelium, 2–3 days post tamoxifen-induced knockout, n=3 biological replicates, Kolmogorov-Smirnov test) reveals significantly reduced expression of genes related to lipid digestion and fatty acid β-oxidation in *Hnf4α γ*$^{DKO}$. Heatmaps of RNA-seq data show (D-E) decreased transcript levels of mitochondrial and peroxisomal β-oxidation genes but (F) increased transcript levels of lipogenesis genes in *Hnf4α γ*$^{DKO}$ (n=3 biological replicates, FDR < 0.05). Asterisks indicate genes that are directly bound by HNF4 within 50kb of annotated TSSs by ChIP-seq. (G) ChIP-seq (n=2 biological replicates) and RNA-seq (n=3 biological replicates) tracks show that HNF4 factors bind to and activate *Acsl5* (acyl-CoA synthetase gene), and loss of HNF4 results in reduced active chromatin signal (H3K27ac ChIP-seq, n=2 biological replicates, see black

dashed rectangles). (H) HNF4 factors can also bind to and activate *Abcd1* (peroxisomal β-oxidation related transporter). The neighboring gene locus is not bound by HNF4 and shows no change in expression levels, serving as an internal control (*Bcap31*, see gray dashed rectangles). More examples are shown in Fig. S2. (I) $Hnf4a\gamma^{DKO}$ mice show decreased FAO activity in both villus and crypt cells. The FAO assay measures palmitoyl-CoA-induced oxidation, as detected by NADH generation. Data are presented as mean ± SEM (villus, n=9 biological replicates; crypt, n= 3–5 biological replicates; Student's t-test, two-sided at $P < 0.05$*). (J) TCA metabolites are reduced upon HNF4 loss. Metabolites were extracted from villus cells scraped from proximal small intestine of $Hnf4a\gamma^{DKO}$ and their WT littermates after 3 consecutive days of tamoxifen or vehicle injection, respectively. Corrected ion counts were normalized by tissue weight, and further normalized relative to the average abundance of metabolite from WT littermates of the same experimental batch. Data are presented as mean ± SEM (LC-MS, n=10 WT and 9 mutants, Student's t-test, two-sided at $P < 0.01$** and $P < 0.05$*).

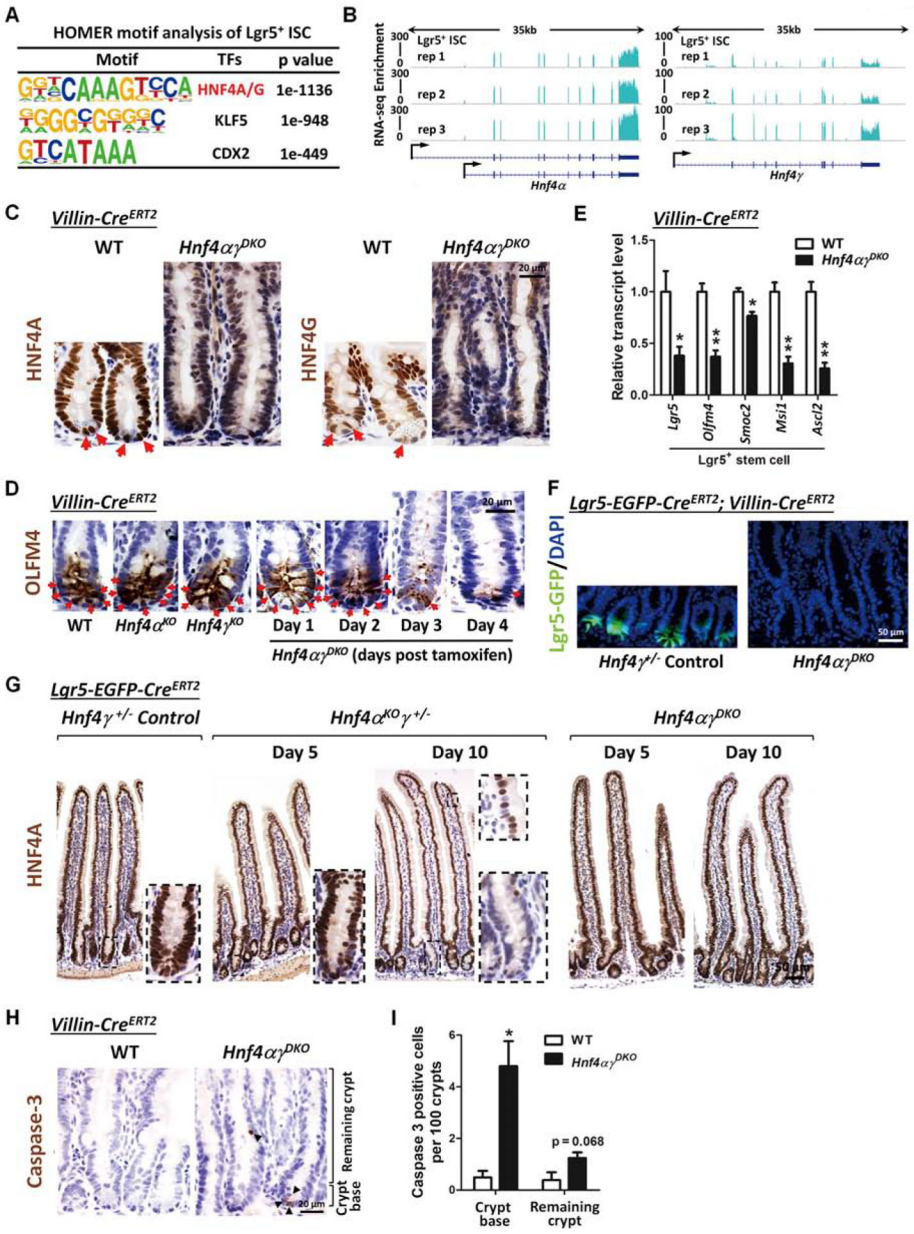


**Figure 3. Loss of HNF4 paralogs in the intestinal epithelium triggers Lgr5$^{+}$ stem cell loss.**

(A) ATAC-seq of isolated intestinal stem cells reveals that HNF4A and HNF4G DNA-binding motifs (HOMER *de novo*) are most abundant at accessible chromatin regions of intestinal stem cells (GSE83394, n=2 biological replicates). (B) RNA-seq tracks of *Hnf4α* and *Hnf4γ* transcript levels in the intestinal stem cells (GSE83394, n=3 biological replicates) show robust expression of these paralogs. (C) Immunostaining of HNF4A and HNF4G in WT and *Hnf4αγ$^{DKO}$* (representative of 3 biological replicates). (D) Immunostaining of OLFM4 (stem cell marker). Stem cells (red arrows) are lost in the crypts following *Hnf4α* and *Hnf4γ* double knockout. (E) qRT-PCR shows a significant decrease in the Lgr5$^{+}$ stem cell markers in *Hnf4αγ$^{DKO}$*. Crypts were isolated from duodenal epithelium of *Hnf4αγ$^{DKO}$* and their WT littermates after 2 consecutive days of tamoxifen or vehicle

injection, respectively. qPCR data are presented as mean ± SEM (n=3 biological replicates, Student's t-test, two-sided at $P < 0.01$** and $P < 0.05$*). (F) Lgr5-GFP$^{+}$ cells are observed in the crypt bottom of control mice, but are completely lost in *Hnf4aγ*$^{DKO}$ after 4 days of tamoxifen-induced knockout (representative of 3 biological replicates). (G) Immunostaining of HNF4A shows that Cre-mediated recombination of the *Hnf4a* locus is initiated via *Lgr5-EGFP-Cre*$^{ERT2}$ ( a stem cell-specific Cre driver).However, most recombined HNF4A-negative cells are not preserved in the epithelium of the *Hnf4aγ*$^{DKO}$ mice (representative of 3 biological replicates), suggesting that *Hnf4aγ*$^{DKO}$ mutant stem cells are replaced by neighboring cells. (H) Immunostaining of cleaved Caspase-3 in WT and *Hnf4aγ*$^{DKO}$. (I) *Hnf4aγ*$^{DKO}$ shows a significant increase of cleaved Caspase-3 postive cells in the crypt base of *Hnf4aγ*$^{DKO}$ compared to WT littermates. Data are presented as mean ± SEM (n=3–4 biological replicates, Student's t-test, two-sided at $P < 0.05$*).

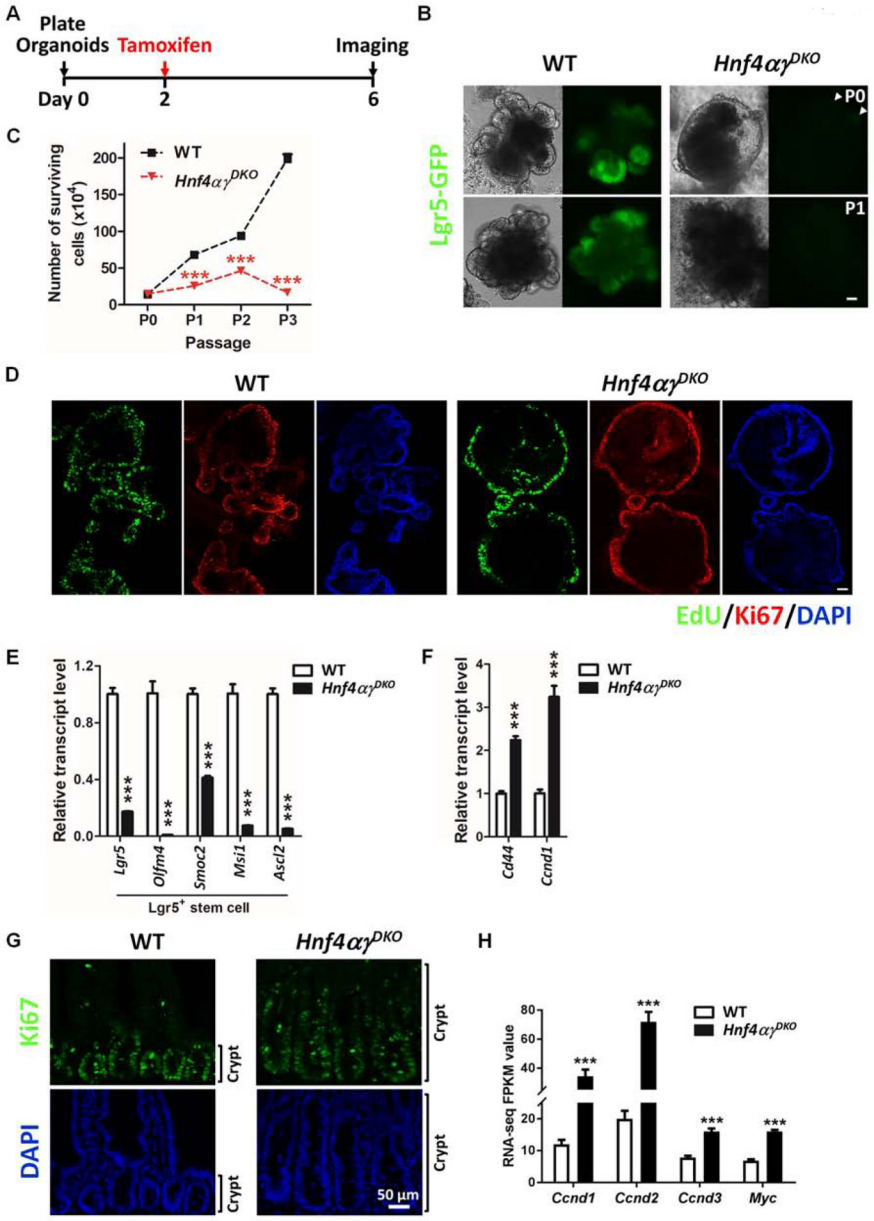


**Figure 4. Transit amplifying-like proliferating cells predominate in the absence of Lgr5$^+$ cells upon HNF4 loss.**

(A) WT organoids exhibit branched structures and express robust Lgr5-GFP, whereas *Hnf4αγ*$^{DKO}$ organoids form spherical structures and exhibit little Lgr5-GFP fluorescence (see arrows). 1 μM tamoxifen or vehicle control was added to culture medium of primary organoids on Day 2 after seeding. After passage, *Hnf4αγ*$^{DKO}$ organoids failed to survive (n=6 independent experiments). Scale bar, 50 μm. Tamoxifen-induced Cre-only controls were also tested and shown in Fig. S4F. (B) WT and *Hnf4αγ*$^{DKO}$ organoids were passaged three times, and the number of surviving cells of organoids (n=4 independent organoid cultures) was counted at each passage, from primary (P0) passage to the third passage (P3). While HNF4 double-mutant organoids grow initially as proliferative spheres, they cannot be passaged indefinetly, such as their control counterparts. (C) Co-staining of EdU and Ki67

(proliferative markers). Organoids were treated with 10 μM EdU 6 hours prior to fixation. Scale bar, 50 μm. qRT-PCR shows a significant decrease of $Lgr5^{+}$ stem cell markers (D) but a significant increase of proliferative cell markers (E) in $Hnf4a\gamma^{DKO}$ organoids. 1 μM tamoxifen or vehicle control was added to culture medium of primary organoids on Day 2 after seeding. All the primary organoids were harvested at Day 6 after seeding. Data are presented as mean ± SEM (n=3 independent organoid cultures, Student's t-test, two-sided at $P < 0.001$***). (F) Crypt elongation is observed in $Hnf4a\gamma^{DKO}$ at day 4 post tamoxifen-induced knockout as shown in Ki67 immunofluorescent staining (representative of 4 biological replicates). (G) RNA-seq data reveal an elevation of proliferative cell markers in $Hnf4a\gamma^{DKO}$ compared to their littermate controls (n=3 biological replicates). Statistical tests were embedded in Cuffdiff at FDR < 0.001***.

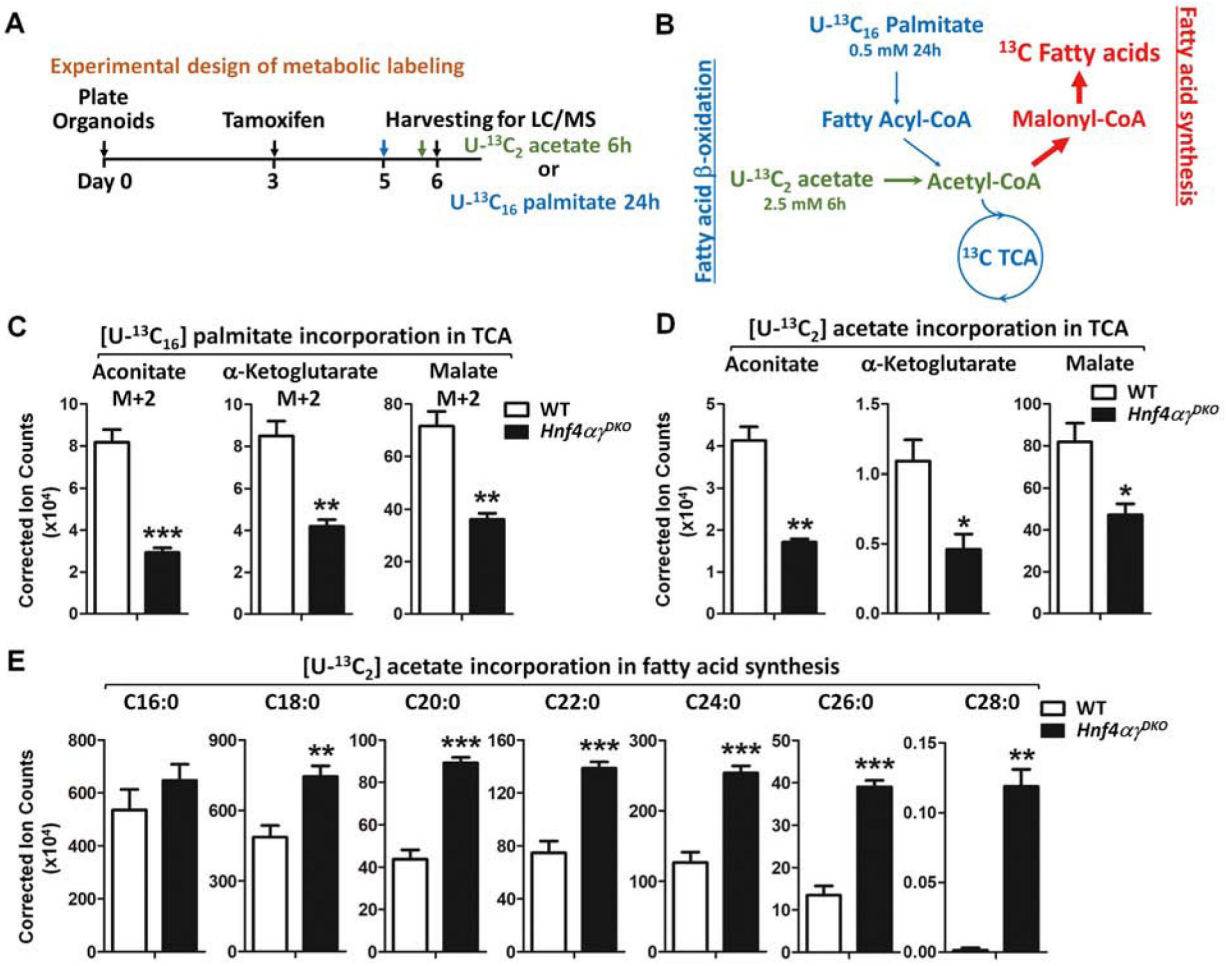


**Figure 5. Loss of HNF4 paralogs leads to compromised TCA cycle contribution and elevated fatty acid synthesis.**

(A-B) Schematics of $^{13}C$ metabolic labeling experiments. (C) 24 hours of labeling with U-$^{13}C_{16}$ palmitate (0.5 mM) indicates reduced contribution of β-oxidation to the TCA cycle metabolites in *Hnf4αγ*$^{DKO}$ organoids (n=4 independent organoid cultures, LC-MS, see expanded panels in Fig. S5A). (D-E) 6 hours of U-$^{13}C_2$ acetate (2.5 mM) labeling shows (D) reduced $^{13}C$ labeled TCA metabolites and (E) elevated $^{13}C$ labeled fatty acids upon HNF4 loss (n=4 independent organoid cultures). Data are presented as mean ± SEM (Student's t-test, two-sided at $P < 0.001$***, $P < 0.01$** and $P < 0.05$*).

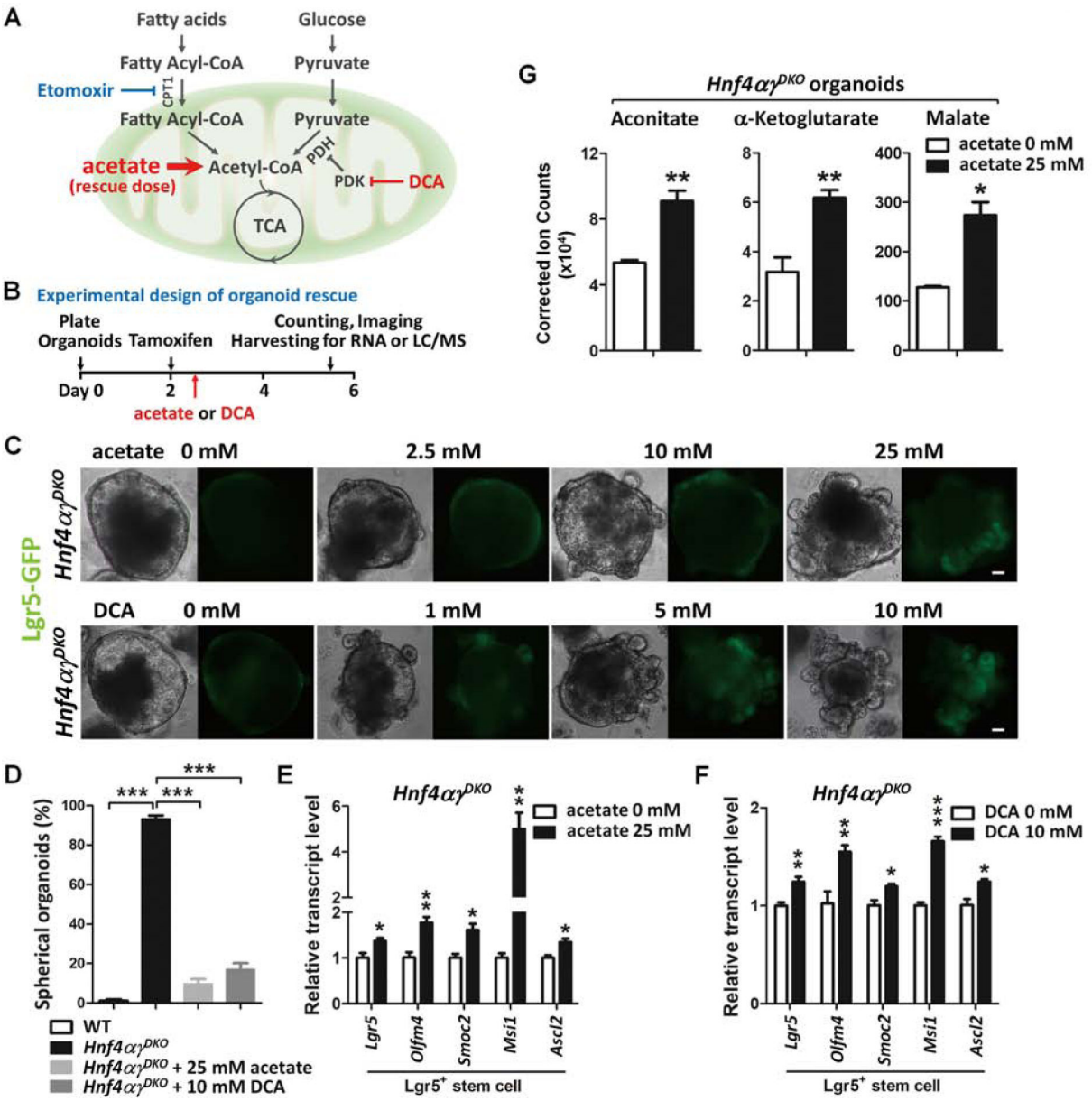


**Figure 6. Acetate supplementation restores TCA cycle metabolites and ISC renewal.**

(A) Schematic of agonists/antagonists used in the fatty acid/pyruvate oxidation-TCA pathways. CPT1: Carnitine palmitoyltransferase I; PDH: Pyruvate dehydrogenase; PDK: Pyruvate dehydrogenase kinase. (B) Schematics of acetate/DCA rescue experiments. (C-F) In *Hnf4αγ*$^{DKO}$, intestinal stem cell maintenance is prolonged with addition of acetate (a precursor of acetyl-CoA) or dichloroacetate (DCA, a promoter of pyruvate oxidation and generation of acetyl-CoA). (C) Representative morphology (n=4 independent experiments) and (D) percentage of spherical organoids arising from organoid culture of *Hnf4αγ*$^{DKO}$ with or without acetate or DCA treatment (n=4 independent organoid cultures, one-way ANOVA followed by Dunnett's post test at $P < 0.001$***). qRT-PCR shows rescued Lgr5$^{+}$ stem cell markers in the *Hnf4αγ*$^{DKO}$ organoids upon (E) 25 mM acetate treatment (n=3 independent organoid cultures) or (F) 10 mM DCA treatment (n=4 independent organoid cultures). (G)

TCA metabolite levels are restored in 25 mM acetate treated *Hnf4a*$\gamma^{DKO}$ organoids (n=4 independent organoid cultures). Scale bars, 50 μm.